Supporting Information

GSH/pH dual-activated POM@MOF for tumor cell-specific synergistic photothermal and chemodynamic therapy

Bole Li[†a], Zhujun Wu[†b], Xiaotong Xu[a], Yanfei Lv[a], Yunfei Guo[a], Siyu Liang[a], Zhimin Wang*[b], Lei He*[a] and Yu-Fei Song*[a].

[a]State Key Laboratory of Chemical Resource Engineering, Beijing University of Chemical Technology, Beijing 100029 P. R. China
[b]Advanced Research Institute of Multidisciplinary Science, Beijing Institute of Technology, Beijing, 100081 P. R. China
Email: helei@mail.buct.edu.cn, zmwang@bit.edu.cn, songyf@mail.buct.edu.cn; Fax/Tel: +86 10 64431832

Table of Contents

Experimental Section
1. Materials
2. Preparations of P@M
3. Physicochemical Characterization
4. Photothermal Properties of P@M
5. Fe^{2+} release assay
6. ·OH Generation by MIL-101-Mediated Fenton Reaction
7. ESR measurements
8. In vitro cytotoxicity evaluation
9. Cell imaging
10. Apoptosis assay
11. *In vivo* safety assay
Supplementary Figures S1-S14
Supplementary Table S1
References

1. Materials

$FeCl_3 \cdot 6H_2O$, terephthalic acid, $H_3PMo_{12}O_{40}$, 1,10-Phenanthroline, 3,3',5,5'-tetramethylbenzidine, 1,2-diaminobenzene, 5,5-dimethyl-1-pyrroline N-oxide and L-glutathione were obtained from Energy Chemical. Dulbecco's modified Eagle's medium (DMEM), fetal bovine serum (FBS), penicillin, and streptomycin were obtained from Gibco. 30% H_2O_2 solution was obtained from Beijing Tongguang Fine Chemicals Company. Cell counting kit-8 (CCK-8), 2',7'-dichlorodihydrofluorescein diacetate (DCFH-DA) Fluorescein isothiocyanateannexin V (Annexin V-FITC), calcein acetoxymethyl ester (calcein-AM), and propidium iodide (PI) chromophore were purchased from Beijing Solarbio Science and Technology Co., Ltd (Beijing, China). All aqueous solutions were prepared in ultrapure water, obtained from a Millipore MilliQ water purification system (Millipore, Billerica, MA USA).

2. Preparations of P@M

$FeCl_3 \cdot 6H_2O$ (2.48 mmol, 0.675 g) and terephthalic acid (1.24 mmol, 0.206 g) were dissolved in 15 mL DMF. After sonicating for 30 min, 0.3 g of $H_3PMo_{12}O_{40}$ was added to the mixture. The solution was then transferred to 100 mL of polytetrafluoroethylene autoclave for 24 h hydrothermal reaction at 110°C. The products were washed 5 times with DMF and ethanol, respectively, and dried under vacuum at 60°C.

3. Physicochemical Characterization

SEM system (Zeiss Supra 55) was used to investigate the morphology and microstructure of the synthesized materials. The elemental composition was analyzed by SEM mapping. Zeta potential and hydrodynamic size were determined by Malvern instrument (Zetasizer Nano ZS). XPS spectra were measured through Shimadzu/Krayos AXIS-Ultra DLD photoelectron spectrometer. XRD patterns were obtained using a LabX XRD-6100 (Shimadzu, China). ICP-OES (ICAP-6300) was used to determine the content of Mo and Fe elements in the synthesized materials. FT-IR spectra were measured using a Bruker VERTEX 70v spectrometer. UV-vis absorption spectra were observed by a TU-1901 spectrophotometer (Persee, Beijing, China). Cell viability was detected by the enzyme labeling apparatus (BioTek Cytation3, USA). The confocal fluorescent images were obtained with Zeiss LSM 800 confocal laser scanning microscope or Nikon Ti2 confocal laser scanning microscope. The induction of apoptosis in HepG2 cells was examined by a fluorescence-activated cell sorting (FACS) Calibur flow cytometer (BD Biosciences).

4. Photothermal Properties of P@M

To investigate the photothermal behavior of P@M, the temperature elevation of POM solution

was recorded, with varied concentrations, laser power densities (at 808 nm) and different pH/GSH concentrations. Also, the photothermal stability of P@M during heating and cooling cycles was tested.

The photothermal conversion efficiency (η) was calculated by following equation:

$$\eta = \frac{hS(T_{max} - T_{sur}) - Q_{dis}}{I(1 - 10^{-A})} \qquad (1)$$

where η referred to the conversion efficiency from 808 nm laser to heat. T_{Max} was the equilibrium temperature and T_{Sur} was the ambient temperature. Q_{Dis} was the baseline energy generated by quartz cell and water upon laser irradiation which could be calculated independently. I was incident laser power. A was the absorbance of POM at 808. S was the surface area of cell and h was heat transfer coefficient. hS was calculated from substituting equations:

$$\theta = \frac{T - T_{sur}}{T_{max} - T_{sur}} \qquad (2)$$

θ was the driving force temperature.

$$t = -\tau_s ln\theta \qquad (3)$$

τ_s was the time constant in cooling period.

$$hS = \frac{mc}{\tau_s} \qquad (4)$$

where m and c were the mass and specific heat capacity of pure water, respectively.

5. Fe^{2+} release assay

P@M was dispersed in PBS buffer with GSH concentrations ranging from 0~20 mM. The pH value of PBS buffer was 7.4, 6.5, 5.5 and 4.8. The concentration of P@M was maintained at 1 mg·mL^{-1}. The released Fe^{2+} was collected and mixed with the Fe^{2+} probe, 1,10-phenanthroline solution (50 μL, 100 mM), for 15 minutes. 1,10-phenanthroline reacted with Fe^{2+} to form a complex with an absorbance at 512 nm. UV-visible absorption was measured to evaluate the amount of released Fe^{2+}.

6. ·OH Generation by MIL-101-Mediated Fenton Reaction

Different concentrations of GSH were added to a 10 mM PBS buffer (pH 5.0) containing 0.8 mM TMB, 10 mM H_2O_2 and 1 mg·mL^{-1} P@M. The oxidation of TMB induced by ·OH was observed by monitoring the change in absorbance at 652 nm. Similarly, the pH effect on ·OH generation was investigated by changing the pH value of PBS buffer.

7. ESR measurements

Qualitative and quantitative analysis of ROS production was conducted using an ESR spectrometer with a center field of 3450 G and 1.0-mm quartz tubes. DMPO, dispersed in water,

was utilized as a probe to detect ·OH radicals. To detect ·OH, P@M (1 mg·mL^{-1}) and DMPO (10 μL, 0.8 M) were mixed in PBS (1 mL) along with H_2O_2 (10 μL, 0.8 M). The experiments were performed at various GSH concentrations (0, 5, 10, 20 mM) and temperatures (25, 37, 47, 55°C).

8. In vitro cytotoxicity evaluation

Human hepatoma cells (HepG2) were cultured in DMEM medium supplemented with 10% FBS and 1% penicillin/streptomycin (PS) and maintained in a humidified cell culture incubator at 37 °C and with 5% CO_2.

Cytotoxicity evaluation of P@M was performed on HepG2 cells *via* the standard CCK-8 assay. Firstly, HepG2 cells were seeded in a 96-well plate, which was incubated at 37°C for 24 h. After removal of the medium and rinsing with PBS, HepG2 cells were pretreated with P@M (final concentration contains 0, 30, 60, 125, 250, 500 or 1000 μg·mL^{-1}) solutions. The cells were incubated for 12 h, followed by addition of CCK-8 (10 μL) for additional 4 h incubation. The absorbance of CCK-8 was measured on a microplate reader at 450 nm. The control group cells (without nanomaterials) were considered to be 100% of survival rate. The cell viability was then determined *via* the following equation: cell viability (%) = (mean of abs. value of treatment group/mean abs. value of control) × 100%. The therapeutic effect of P@M was further studied. Briefly, HepG2 cells were treated with (i) P@M+NIR, (ii) P@M+H_2O_2, and (iii) P@M+NIR+H_2O_2. The content of P@M in these groups were 0, 12, 25, 50, 100, 200 μg·mL^{-1}. Groups (ii) and (iii) were irradiated with an 808 nm laser (1.0 W·cm^{-2}) for 5 min. Subsequent treatments were conducted with the same experimental conditions as mentioned above.

9. Cell imaging

HepG2 cells were seeded in a six-well plate at an initial density of 1 × 10^5 cells per well. Then, the cells were treated with different formulations: (i) control, (ii) H_2O_2, (iii) P@M, (iv) P@M + H_2O_2, (v) P@M + NIR and (vi) P@M + NIR + H_2O_2. The content of P@M in groups (iii), (iv), (v) and (vi) was 200 μg·mL^{-1}. After 24 hours of incubation, group (v) and (vi) were irradiated by 808 nm laser irradiation (1.0 W·cm^{-2}) for 20 min.

For in vitro ROS detection, after accepting the above treatments, HepG2 cells were stained with a fluorescent ROS probe (DCFH-DA: 20 μM, 1 mL) for 20 min. The cell fluorescence images were performed by a CLSM with 488 nm laser excitation.

For live/dead cell staining, the treated HepG2 cells were stained with Calcein AM (2 μM) and PI (4 μM) for 15 min. After fixing the cells with glutaraldehyde and washing them with PBS, all fluorescence images were acquired via CLSM.

10. Apoptosis assay

HepG2 cells were seeded in a six-well plate at an initial density of 1×10^5 cells per well. After 24 hours of cell adhesion, the cells were treated with the following: (i) control, (ii) P@M, (iii) P@M + NIR, (iv) P@M + H_2O_2 and (v) P@M + NIR + H_2O_2. The content of P@M in groups (ii), (iii), and (iv) was 200 μg·mL^{-1}. Groups (iii) and (v) were irradiated with an 808 nm laser (1.0 W·cm^{-2}) for 20 min. All treated cells were trypsinized, washed, and quantified by an annexin V-FITC/PI apoptosis detection kit.

11. *In vivo* safety assay

Male BALB/c mice were intravenously injected with P@M at a dose of 20 mg·kg^{-1}. After administration, the blood samples were collected for blood biochemistry and complete blood panel analysis. Major organs (heart, liver, spleen, lung and kidney) were dissected, fixed in 4% paraformaldehyde solution and stained with hematoxylin and eosin (H&E) for histological analysis.

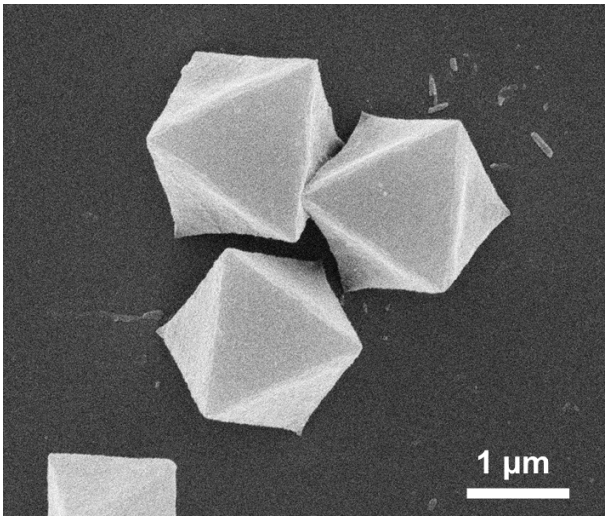

Figure S1. SEM image of MIL-101.

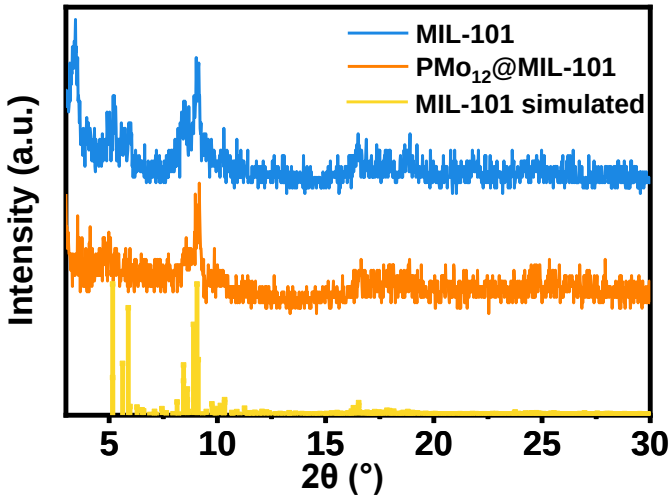

Figure S2. XRD pattern of P@M and MIL-101.

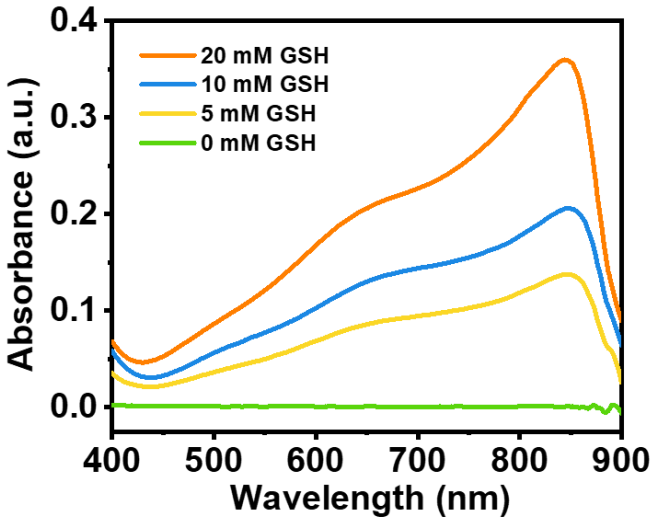

Figure S3. UV-vis spectra of PMo_{12} in pH 5.5 buffer with different GSH concentrations.

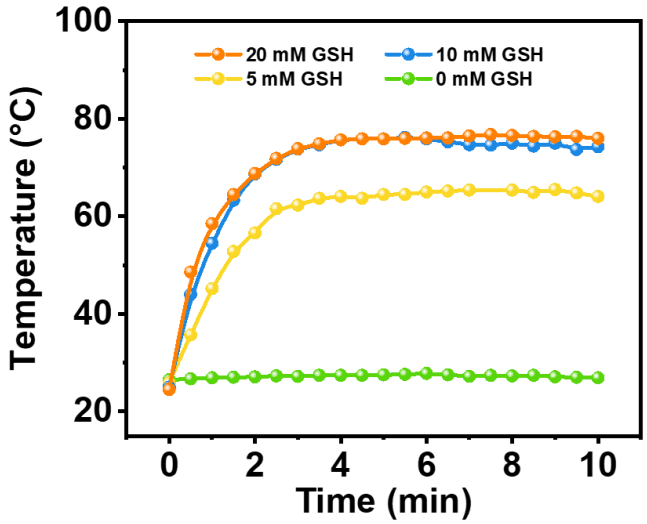

Figure S4. Temperature evaluation of P@M under different GSH concentrations with the irradiation of 808 nm laser (1.0 W·cm^{-2}) for 10 min.

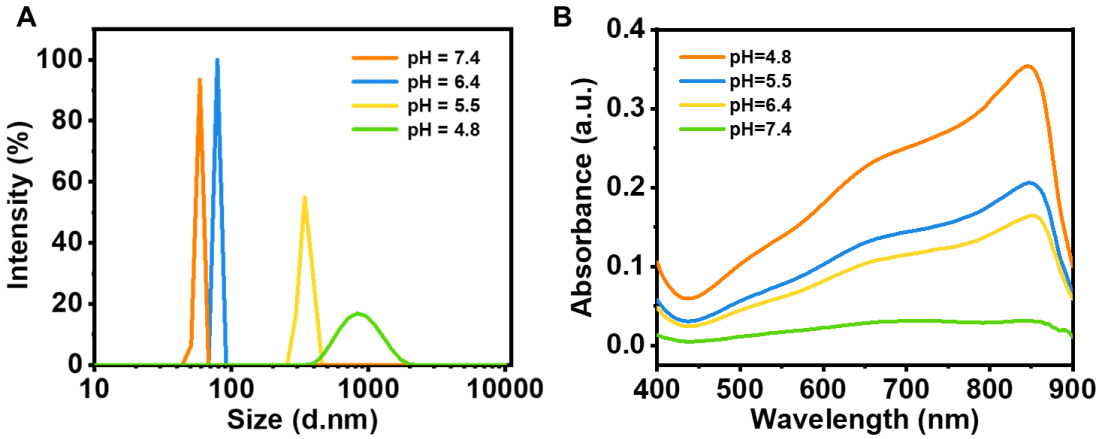

Figure S5. A) DLS distribution of PMo_{12} at different pH values. B) UV-vis spectrua of PMo_{12} in different pH values. GSH concentration was 10 mM.

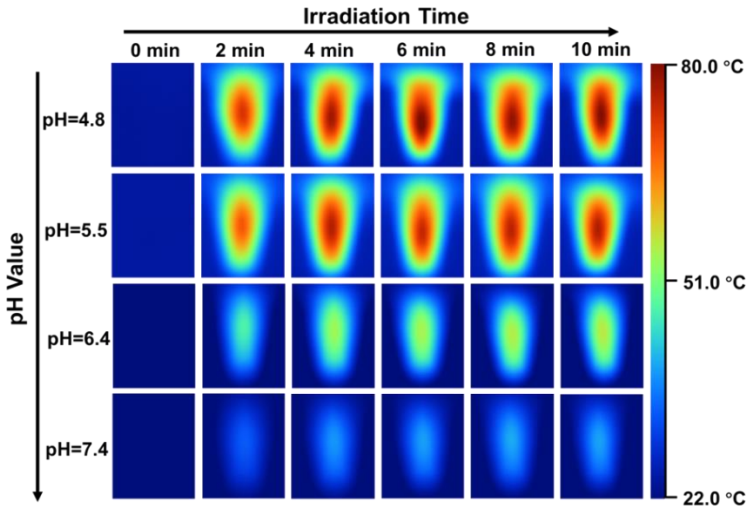

Figure S6. Infrared thermal images of 1mg/mL P@M in different pH values within 10 min-irradiation under 808 nm (1 W/cm^2) when GSH concentrations is 10 mM.

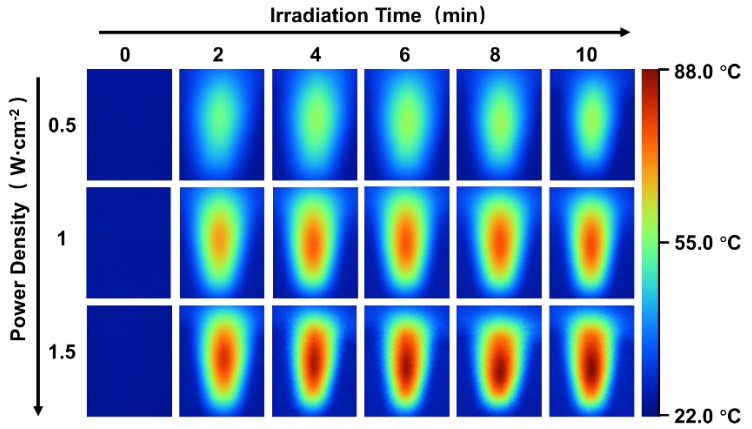

Figure S7. Infrared thermal images of 1mg/mL P@M at different power densities over 10 min-irradiation under 808 nm when GSH concentrations is 10 mM and pH value is 5.5.

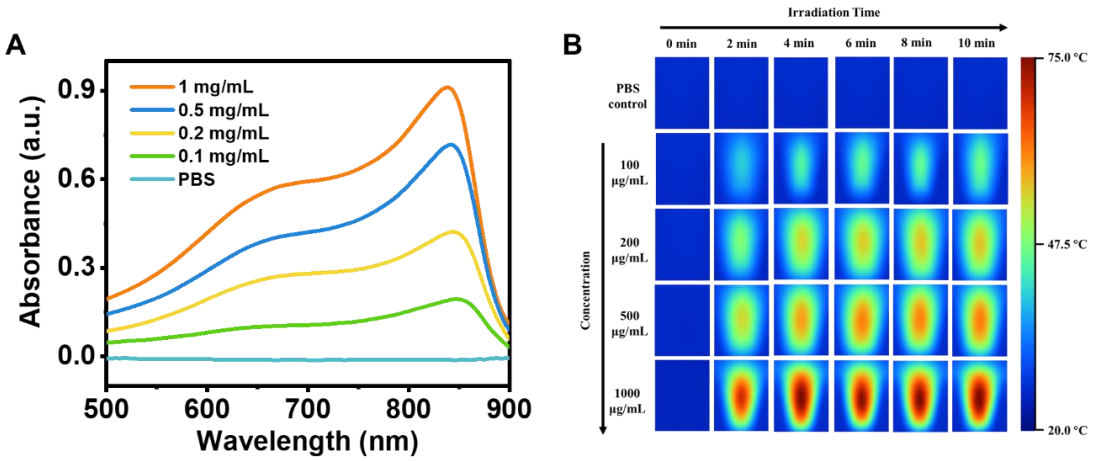

Figure S8. A) UV-vis spectra of P@M at different concentrations in pH 5.5 buffer with 10 mM GSH. B) Infrared thermal images of P@M at different concentrations within 10 min-irradiation under 808 nm.

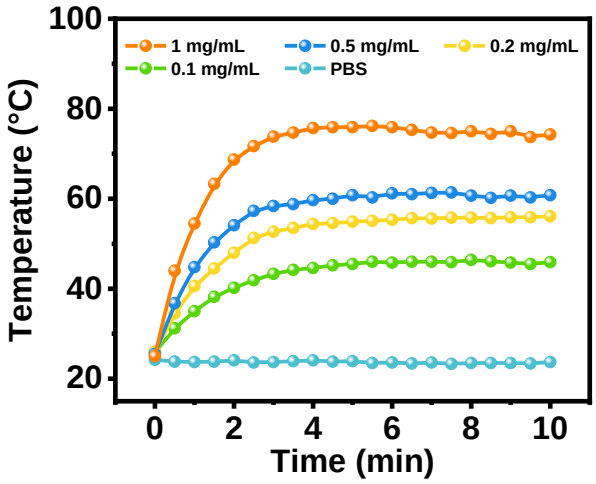

Figure S9. Temperature evaluation of different concentrations P@M when the pH value is 5.5 and GSH concentrations is 10 mM under the irradiation of 808 nm laser (1.0 W·cm^{-2}) for 10 min.

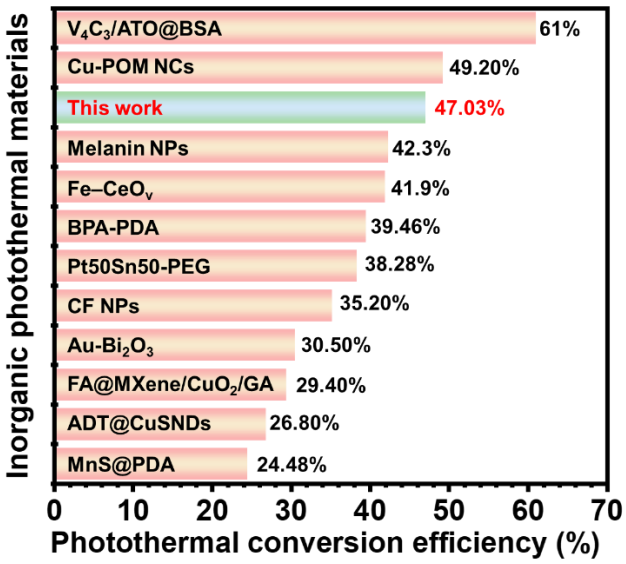

Figure S10. Photothermal conversion efficiencies of the inorganic photothermal materials in some representative reports[1-11].

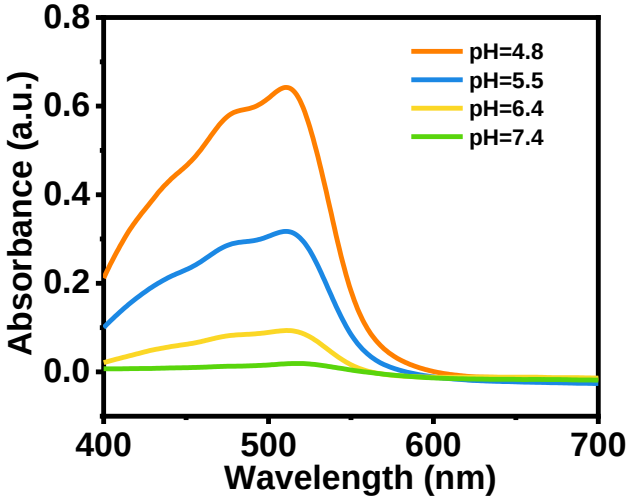

Figure S11. UV-vis spectra of P@M with o-phenanthroline at different pH values.

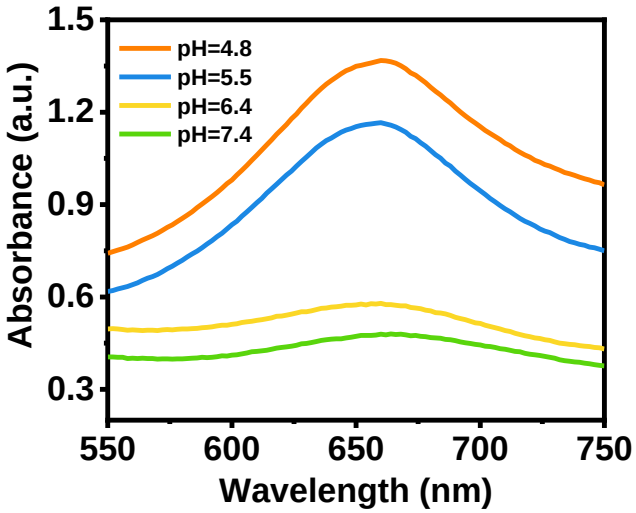

Figure S12. UV-vis spectra of P@M in different pH conditions with TMB under 100 μM H_2O_2.

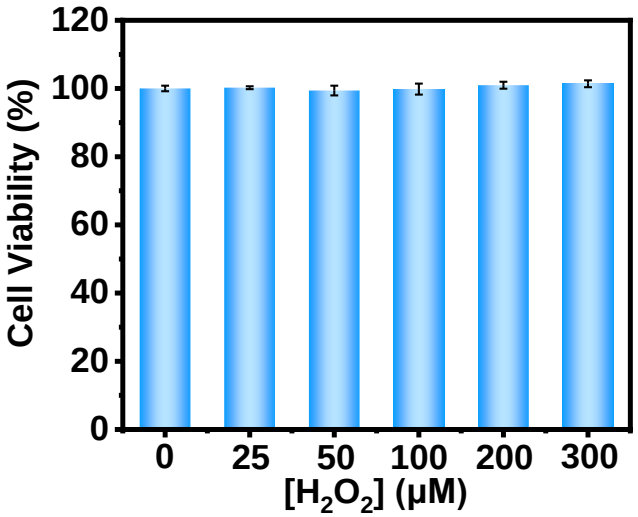

Figure S13. Cytotoxicity of H_2O_2 in HepG2 cells.

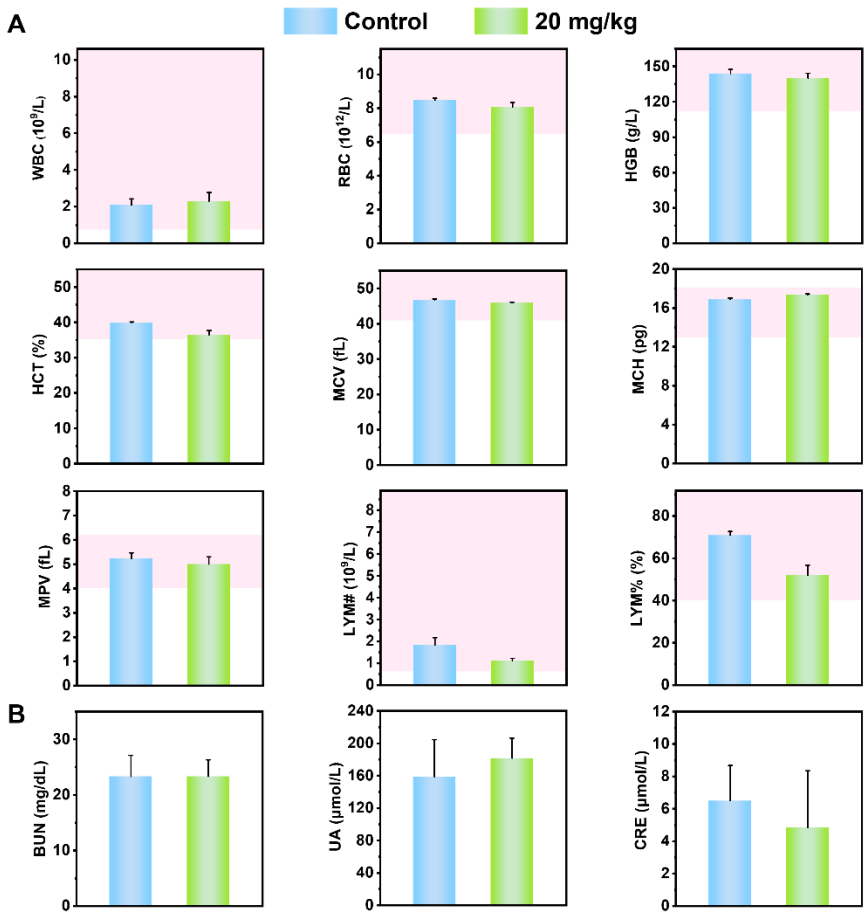

Figure S14. A) Blood routine and B) blood biochemistry examinations of mice after receiving intravenous injections with P@M.

Table S1. ICP result of P@M.

Fe (ppm)	Mo (ppm)	Calculated PMo_{12} content (wt%)
0.4493	0.4337	26.8%

References

1 G. Ma, X. Zhang, K. Zhao, S. Zhang, K. Ren, M. Mu, C. Wang, X. Wang, H. Liu., J. Dong and X. Sun, Polydopamine Nanostructure-Enhanced Water Interaction with pH-Responsive Manganese Sulfide Nanoclusters for Tumor Magnetic Resonance Contrast Enhancement and Synergistic Ferroptosis-Photothermal Therapy, *ACS Nano*, 2024, **18**, 3369-3381.

2 J. Cheng, Y. Zhu, Y. Dai, L. Li, M. Zhang, D. Jin, M. Liu, J. Yu, W. Yu, D. Su, J. Zou, X. Chen and Y. Liu, Gas-Mediated Tumor Energy Remodeling for Sensitizing Mild Photothermal Therapy, *Angew. Chem. Int. Ed.*, 2023, **62**, e202304312.

3 P. Xiong, X. Wei, L. Zhou, W. Zhou, M. Li, Y. Ge, J. Zou, S. Peng, L. Jiang, L. Tian and Y. Liu, Near-Infrared Light-Triggered MXene Nanocomposite for Tumor-Specific Mild Photothermal-Enhanced Chemodynamic Therapy, *Adv. Funct. Mater*. 2024, 2405124.

4 G. Chen, J. Du, L. Gu, Q. Wang, Q. Qi, X. Li, R. Zhang, H. Yang, Y. Miao and Y. Li, Metal-sensitized Au-Bi_2O_3 nanoheterojunction for immunogenic cell death-boosted sono-immuno cancer therapy, *Chem. Eng. J.*, 2024, **482**, 148953.

5 X. Wei, R. Han, Y. Gao, P. Song, Z. Guo, Y. Hou, J. Yu and K. Tang, Boosting Energy Deprivation by Synchronous Interventions of Glycolysis and Oxidative Phosphorylation for Bioenergetic Therapy Synergetic with Chemodynamic/Photothermal Therapy, *Adv. Sci*. 2024, 2401738.

6 Y. Zhu, R. Zhao, L. Feng, C. Wang, S. Dong, M. V. Zyuzin, A. Timin, N. Hu, B. Liu and P. Yang, Dual Nanozyme-Driven PtSn Bimetallic Nanoclusters for Metal-Enhanced Tumor Photothermal and Catalytic Therapy, *ACS Nano*, 2023, **17**, 6833-6848.

7 L. Dai, T. Wang, S. Zhou, L. Pan, Y. Lu, T. Yang, W. Wang and Z. Qian, Boronophenylalanine-Containing Polydopamine Nanoparticles for Enhanced Combined Boron Neutron Capture Therapy and Photothermal Therapy for Melanoma Treatment, *Adv. Funct. Mater.* 2024, 2402893.

8 S. Dong, Y. Dong, Z. Zhao, J. Liu, S. Liu, L. Feng, F. He, S. Gai, Y. Xie and P. Yang, "Electron Transport Chain Interference" Strategy of Amplified Mild-Photothermal Therapy and Defect-Engineered Multi-Enzymatic Activities for Synergistic Tumor-Personalized Suppression, *J. Am. Chem. Soc.*, 2023, **145**, 9488-9507

9 W. Song, Y. He, Y. Feng, Y. Wang, X. Li, Y. Wu, S. Zhang, L. Zhong, F. Yan, L. Sun, Image-Guided Photothermal and Immune Therapy of Tumors via Melanin-Producing Genetically Engineered Bacteria. *Small*, 2024, 2305764.

10 H. Zhao, C. Zhao, Z. Liu, J. Yi, X. Liu, J. Ren, X. Qu, A Polyoxometalate-Based Pathologically Activated Assay for Efficient Bioorthogonal Catalytic Selective Therapy, *Angew. Chem. Int. Ed.*, 2023, **62**, e202303989.

11 R. Zhao, Y. Zhu, L. Feng, B. Liu, Y. Hu, H. Zhu, Z. Zhao, H. Ding, S. Gai, P. Yang, Architecture of Vanadium-Based MXene Dysregulating Tumor Redox Homeostasis for Amplified Nanozyme Catalytic/Photothermal Therapy, *Adv. Mater*. 2024, **36**, 2307115.